Tom Milligan
Milligan & Associates
8204 West Polk Place
Littleton, CO 80123
(303) 977-7268
(303) 977-8853 (Fax)
TMilligan@ieee.org (e-mail)

MAMA: A New Methodically Designed Broadband Microstrip Antenna Using Off-the-Shelf Components

Hassan El Kamchouchi and Gehan Abouelseoud

Alexandria University, Egypt
E-mail: helkamchouchi@ieee.org, dr.yasmine@gmail.com

Abstract

The current paper proposes a new, simple, methodical approach to broadband microstrip antenna design. The approach relies on a reformulation of the antenna-design problem as an impedance-matching problem, in which the antenna is considered to be the matching device required to match the feed line to air. Thus, impedance-matching techniques, such as Chebyshev transformers and a Klopfenstein taper, are employed to determine the antenna parameters necessary to satisfy a set of specifications. Simulation results as well as measured results show that the proposed Matched-to-Air Microstrip Antennas (MAMAs) qualify as a new class of broadband microstrip antennas, which have the advantages of relying on a systematic approach (as opposed to the usual trial-and-error procedures that are now prevalent), as well as being very easy to fabricate, using inexpensive off-shelf components.

Keywords: Microstrip antennas; broadband antennas; impedance matching; Chebyshev functions; Klopfenstein taper; FDTD methods; moment methods

1. Introduction

Despite the advantages of microstrip antennas – including their small size, inexpensive cost, and ability to be integrated with VLSI designs – they have the major disadvantage of low impedance bandwidth (typically 1% to 4 % of the operating frequency). This is a serious limitation for modern wireless communication systems, which tend to strongly support multimedia services, as well as for military applications such as frequency-hopping radars, ground-penetrating radars (GPR), imaging, and other important applications. Thus, it is the primary aim of many microstrip-antenna designers to look for methods to improve the impedance bandwidth [1, 2]. The impedance bandwidth is defined as the range of frequencies for which $|S_{11}| < -10\,\text{dB}$. The difficulty in deriving analytical models for arbitrarily shaped microstrip antennas has led designers to depend mainly on full-wave simulators, based on numerical methods such as the Finite-Difference Time-Domain (FDTD) and the Method of Moments (MoM) to test their intuitive solutions. Thus, most available designs depend on a guess – simulate – redesign cycle, which is more-or-less a trial-and-error design procedure. The present paper suggests an alternative approach to the microstrip-antenna design problem. The broadband antenna is considered to be a device that matches the feed-line impedance to the intrinsic impedance of the air. The authors call this class of antennas matched-to-air microstrip antennas (MAMAs).

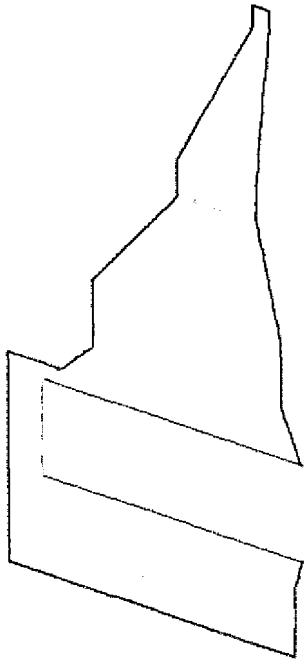

Figure 1. A three-dimensional view of a four-stage MAMA.

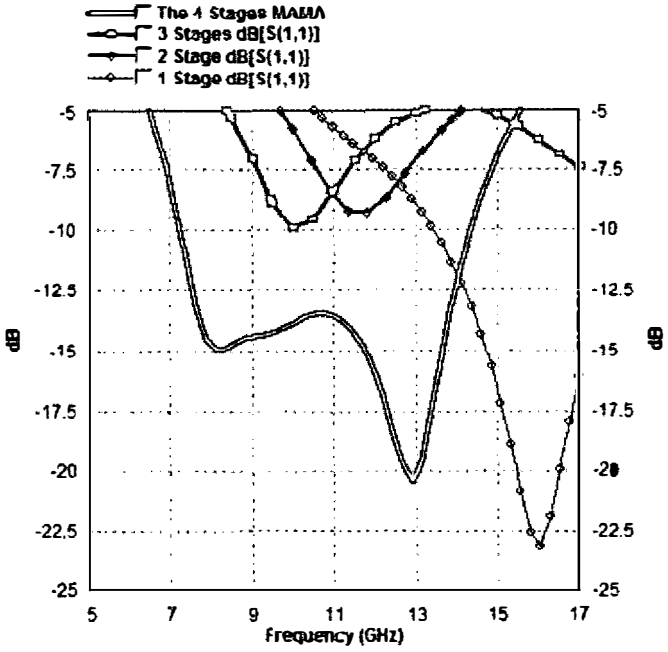

Figure 4. The $|S_{11}|$ parameters of a one section (one stage), two sections (two stages), three sections (three stages), and the whole four-stage MAMA. It was clear that increasing the number of sections gradually improved the antenna's bandwidth.

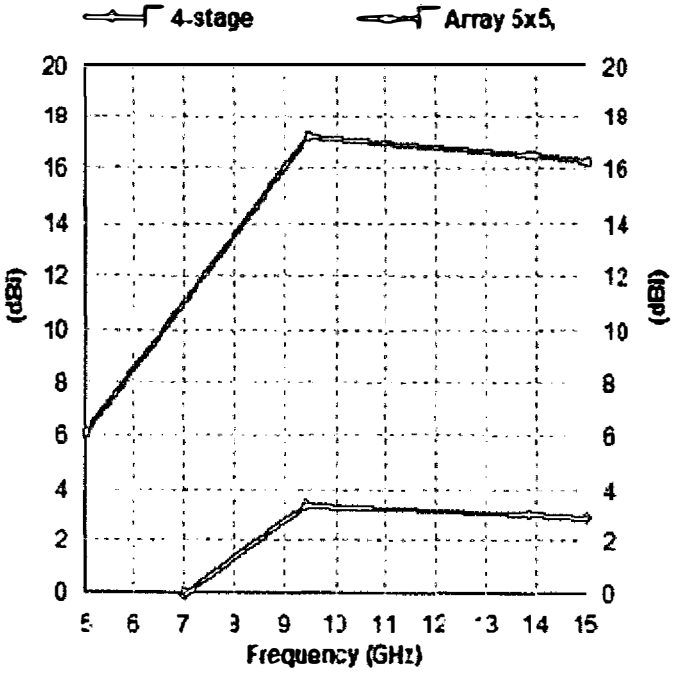

Figure 5. This plot shows how the gain of the proposed MAMA can be enhanced using an array of 5 × 5 elements spaced $\lambda_0/2$ apart.

2. The Design Procedure for MAMAs Based on Chebyshev Transformers

Initially [3], the substrate thickness h is chosen so as to avoid higher modes. Typically, $h < 0.05\lambda_0$, where λ_0 is the wavelength at the design frequency. Based on this thickness and using the formula in [4, 5], a suitable width, w, of the feed line is chosen to design a line with a characteristic impedance of 50 ohms. To simplify the design task, the antennas considered are built on an air substrate, $\varepsilon_r = 1$. (Note that all the formulas used in this paper are simplified based on this). The problem of broadband microstrip-antenna design is then perceived as that of matching the feed-line impedance to the 120π ohm intrinsic impedance of air. Using the Chebyshev multi-section impedance transformer [6], a microstrip antenna has been designed to perform the matching task. Using Chebyshev transformer tables [6], the value of the impedance for each section of the multi-section transformer can be determined so that the maximum reflection coefficient in the pass band does not exceed a certain value, Γ_m. Once the impedance is determined for each section, the patch parameters (patch width, w, length, l, and height, h) corresponding to this impedance are determined so as to satisfy the following three constraints:

1. The characteristic impedance of the patch, modeled as a microstrip line, can be calculated using the Hammerstad and Jensen formula [4],

$$60\log\left[\frac{h}{w}\left\{6+0.2832\exp\left[-\left(30.666\frac{h}{w}\right)^{.7528}\right]\right\} + \sqrt{1+\left(2\frac{h}{w}\right)^2}\right] = fac_i Z_r Z_L,$$

where fac_i is a factor determining the ratio of the impedance of transformer section i to that of the feed line (and is determined using Chebyshev design tables), and $Z_r Z_L$ is the feed-line impedance.

2. The multi-section transformer technique is based on the assumption that the length of each section is $\lambda_0/4$. Thus, the effective length of the patch [7] is taken to be $\lambda_0/4$. This leads to the following equation:

$$l + 1.4437h\frac{\frac{w}{h}+0.264}{\frac{w}{h}+0.8} = \frac{75}{f_0}.$$

3. For the patch to be an efficient radiator, the patch width should be $w = 150/f_0$, so the effective width of the patch [2] is equated to this value, giving the third constraint:

$$\frac{150}{f_0} = \frac{2}{\log\left[\frac{h}{w}\left\{6+0.2832\exp\left[-\left(30.666\frac{h}{w}\right)^{.7528}\right]\right\} + \sqrt{1+\left(2\frac{h}{w}\right)^2}\right]}.$$

Solving the three nonlinear equations determines the w, h, l values for each section. The Chebyshev transformer technique was used especially because it is known to give wideband matching. A typical MAMA, designed using this procedure, is shown in Figure 1. It is believed that the simulation results will not be quite as expected, due to the sharp transitions from stage to stage in the Chebyshev design. Thus, to improve the results, the authors tried using the Klopfenstein taper, which is the continuous generalization of the Chebyshev multistage transformer.

3. Results of Chebyshev-Based MAMA

The authors tried several examples, using different numbers of multiple sections. The first example was for an antenna operating at $f = 10$ GHz. The number of sections was taken to be four, with a maximum allowable reflection coefficient of 0.05. This could be considered to be an over-design, to assure broadband performance (the bandwidth was taken to be the range of frequencies for which $|S_{11}| < -10$ dB). All dimensions are in mm. The ground plane size was taken to be 10 mm × 10 mm, and was found to be a critical parameter for enhancing the bandwidth. The width of the feed line was 1.6 mm, and the air substrate height was 0.3 mm (to avoid exciting higher-order modes). The substrate height and feed-line width made the feed-line impedance 47.125 ohms, which was close enough to the 50 ohm standard, and which enabled the authors to deduce the impedance of each section directly from available Chebyshev tables. Solving the nonlinear equations cited above, using a numerical software available online from http://www.numericalmathematics.com, gave the following dimensions for the antenna:

Section 1: $l = 4.5$ mm, $w = 9.1$ mm, $h = 2.4$ mm

Section 2: $l = 3.1$ mm, $w = 6.6$ mm, $h = 3.9$ mm

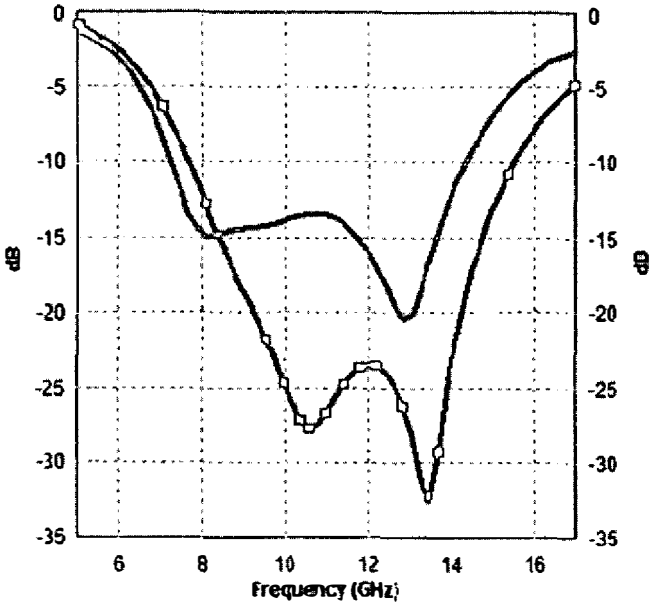

Figure 2. This figure compares the $|S_{11}|$ parameters, in dB, of a four-stage MAMA as calculated using both the *Fidelity* (–□–) and IE3D (——) software packages.

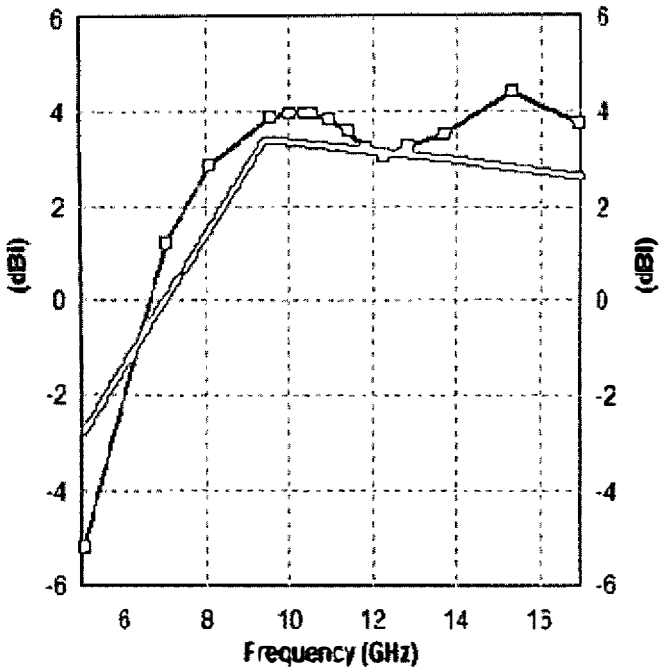

Figure 3. The total field gain of a four-stage Chebyshev MAMA. The gain over the operating band ranged from 2 dBi to 4 dBi, which is typical of microstrip antennas.

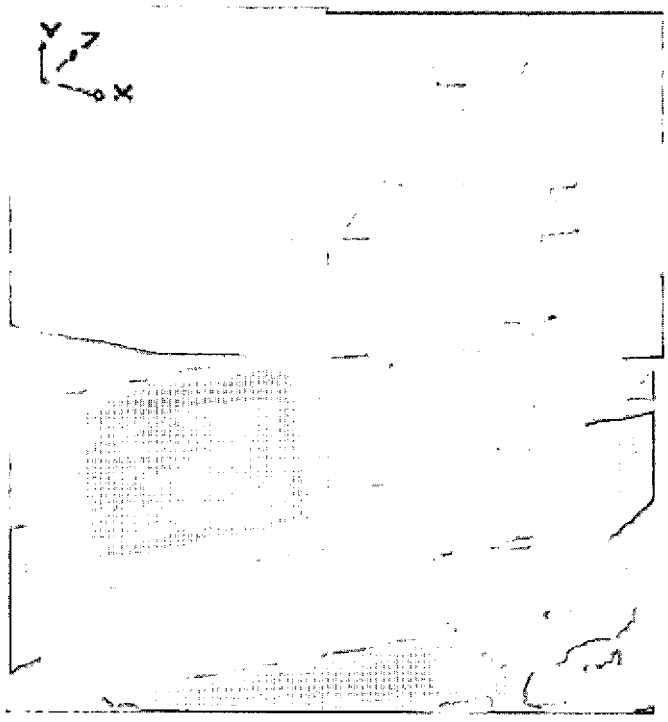

Figure 6. The top two photos show the front and back views of the prototype fabricated four-stage MAMA. The bottom photo shows the return-loss measurement setup. The antenna was connected directly to the network analyzer to avoid cable-induced errors. The measurement procedure was proceeded by a one-port calibration scheme (since the authors were only interested in return-loss measurements).

Section 3: $l = 1.8$ mm, $w = 2.8$ mm, $h = 7.3$ mm

Section 4: $l = 1.1$ mm, $w = 0.65$ mm, $h = 11.9$ mm

All heights were measured from the ground plane. Both the *IE3D* (Method-of-Moments simulator) and *Fidelity* (Finite-Difference Time-Domain) simulators were used to simulate the designed antenna. It is known that no numerical simulator is perfect. Thus, using more than one simulator appears to be necessary for the designer to gain confidence in a prospective approach before moving to the prototyping step.

Figure 2 shows the $|S_{11}|$ parameters. The antenna's bandwidth was nearly 54%. Figure 3 shows the total field gain in dBi, as calculated using both *Fidelity* and *IE3D*. The gain in the operating band ranged from 2 dBi to 4 dBi. Figure 4 shows the simulation results for one section (one stage), two sections (two stages), and three sections (three stages), and the whole MAMA. It was clear that increasing the number of sections gradually improved the antenna's bandwidth. Figure 5 shows how the gain of the proposed MAMA could be enhanced by using an array of 5×5 MAMA elements separated by $\lambda_0/2$.

Figure 6 shows the fabricated practical prototype. To be able to measure the $|S_{11}|$ parameters using the HP 82720B network analyzer, frequency scaling was used to transfer the design point to 1 GHz. The measured return loss compared with the simulation results and the desired practical prototype are shown in Figure 7. The bandwidth obtained was 74.5% of the 1.02 GHz central frequency. The radiation pattern was measured using the Lab-Volt antenna training kit. The differences between the practical and simulated results had several reasonable causes. First, the antenna was manufactured manually, and so it was difficult to achieve precise dimensions, especially for the substrate height at the feed line. Second, the probe available in the lab had slightly different dimensions than those desired (particularly shorter), and attempts to manually solder a longer probe would have inevitably introduced parasitic capacitance. In fact, the simulators used simply modeled the probe feed using a vertically localized port scheme, which considers the feed to result in a uniform field below the feed line at the plane perpendicular to it, and thus the simulators did not capture all feed details. Thirdly, the antenna was built on an air substrate, so it was necessary to include a dielectric rod at the highest patch for support. This rod had an adverse effect on the bandwidth predicted by the authors from simulations. The rod was made of a cheap melted glue material that is usually used with glue guns as an adhesive for wood and plastic. Moreover, at the sides of the first vertical wall, epoxy with a height of 3 mm was used to keep the feed line at the desired height. Of course, a carefully chosen dielectric could have been used to produce a less-adverse effect on performance, but the general motto that initiated our project was "broadband antennas from off-the-shelf components. The general theme of the work was to encourage young designers to exercise their innovative skills, without having to wait for expensive equipment and materials to be available.

The radiation patterns are shown in Figure 8. They were calculated at 1 GHz. However, the authors' investigation of the pattern at other frequencies within the operating range showed that it was as if the pattern rotated slightly with changing frequency. However, because the applications of the antenna are concerned mainly with bandwidth, the shape of the radiation pattern is not of primary importance (indeed, even if it is important, arrays of MAMA elements can be used for radiation-pattern shaping.)

The desired prototype results were based on [6], where, for a Chebyshev-based MAMA,

$$|S_{11}| = 20\log(\Gamma_m T_n),$$

$$T_n = \cos\left[n \operatorname{acos}\left\{ \cos\left(2\pi \frac{f}{f_0}\right) \cosh\left[\frac{1}{n} acosh \frac{\left(\ln \frac{Z_L}{Z_0}\right)}{(2\Gamma_m)} \right] \right\} \right],$$

where n is the number of sections of the Chebyshev transformer.

4. Klopfenstein-Based Mama

As was pointed out earlier, it was believed that one of the reasons for the differences between the practical and prototype results for the Chebyshev-based MAMA was the sharp change from stage to stage. Thus, it is natural to believe that using a tapered patch, such as a Klopfenstein patch, is likely to produce better results. The Klopfenstein taper [8] can be thought of as the limiting case of the Chebyshev transformer when the number of sections approaches ∞. The design procedure based on the Klopfenstein taper can be summarized as follows.

The procedure starts by specifying the maximum-allowable pass-band reflection coefficient, Γ_m, taking into account considerable tolerance, as well as specifying the pass-band starting frequency, f_i. Thus, the length of the patch is determined using the relations

$$\Gamma_0 = \frac{1}{2}\ln\left(\frac{Z_L}{Z_0}\right),$$

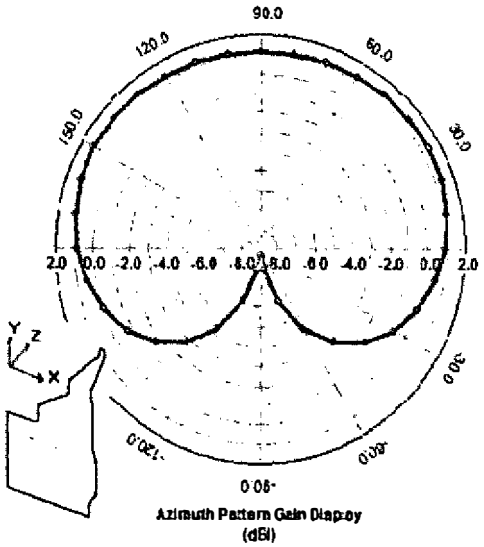

Figure 8a. The radiation pattern in the *xy* plane at 1 GHz. The pattern can be considered omnidirectional, with the effect of the ground plane clear. The authors' simulations showed that the pattern shapes did exhibit some changes over the operating bandwidth. However, the changes in maximum gain and overall shape were acceptable for applications that are mainly concerned with the bandwidth.

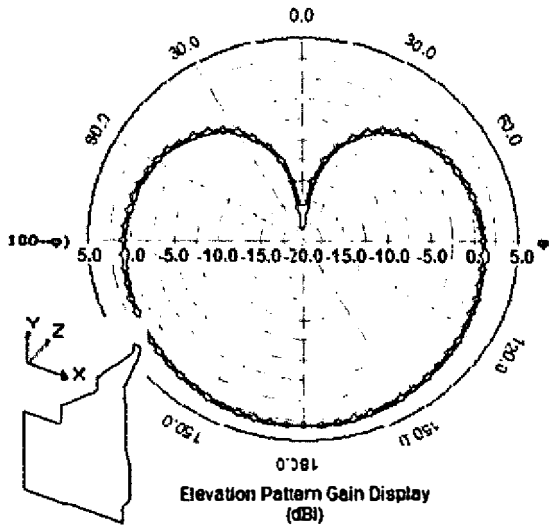

Figure 8b. The radiation pattern in the *xz* plane at 1 GHz. The other comments of Figure 8a apply.

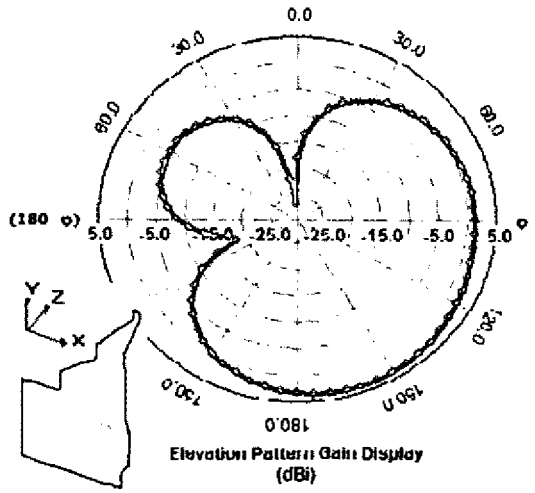

Figure 8c. The radiation pattern in the *yz* plane at 1 GHz. The other comments of Figure 8a apply.

$$A = \cosh^{-1}\left(\frac{\Gamma_0}{\Gamma_m}\right),$$

$$L = 300\frac{A}{(2\pi f_i)},$$

where L is the length of the taper in mm and f_i is the onset of the pass band.

The following equations are then used to derive the impedance profile required to match the feed line to air:

$$\ln Z(y) = \frac{1}{2}\ln(Z_0 Z_l) + \frac{\Gamma_0}{\cosh A} A^2 \Phi\left(\frac{2y}{L} - 1, A\right), \quad 0 \le y \le L$$

$$\Phi(x, A) = -\Phi(-x, A) = \int_0^x \frac{I_1\left(A\sqrt{1-r^2}\right)}{A\sqrt{1-r^2}}\, dr, \quad |x| \le 1.$$

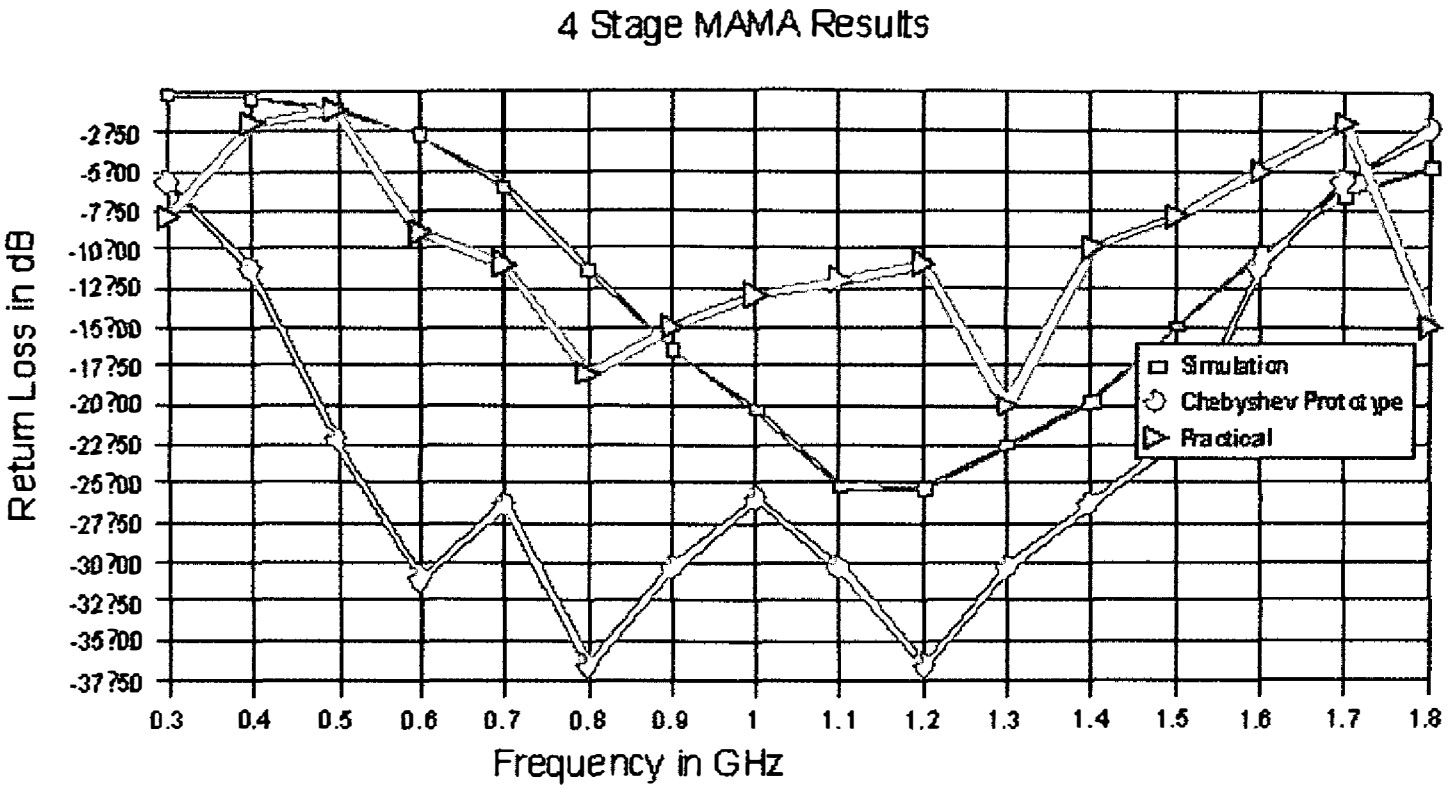

Figure 7. A comparison of the practical and simulated results with the synthesis prototype for a four-stage MAMA. The synthesis prototype had a target of a 130% bandwidth centered at 1 GHz. The simulation results predicted a 76.4% bandwidth centered at 1.1 GHz, while the actual practical results had a 74.5% bandwidth centered at 1.02 GHz. The differences in the locations of the resonance frequencies as well as in the return-loss levels were explained in the parametric study. It was clear from the above figure that increasing the number of stages indeed improved the impedance bandwidth. However, practical experience dictated that the results of the fabricated antenna should be more accurately perceived as two adjacent disjoint bands at 1.2 GHz, because of the narrow match (just –11 dB) at this point, which made this particular frequency sensitive to any variation in measurement settings or surrounding environment. The ground plane size for the four-stage MAMA considered in the figure was 100 mm × 100 mm.

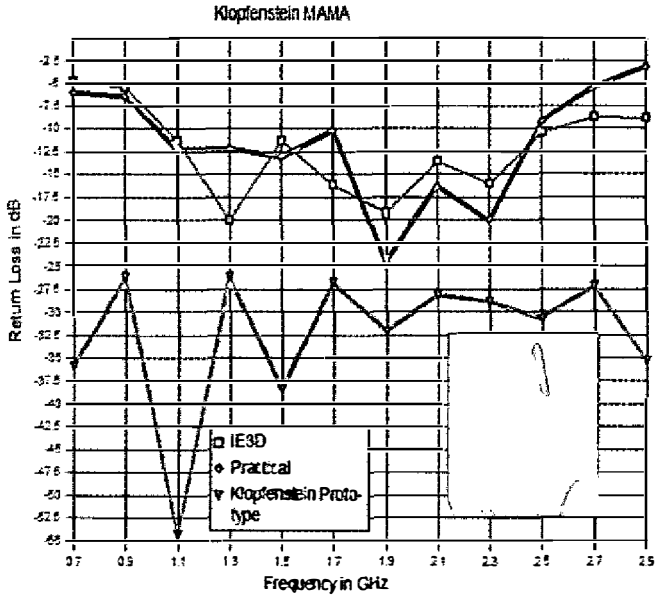

Figure 10. This plot compares the simulated and practical results for the Klopfenstein MAMA prototype. It was clear that in terms of bandwidth size, both the practical and simulation results were in perfect agreement. However, there were differences in the matching levels between the simulated and practical results. The differences may have been due to several reasons, which are explained in the text.

A very simple method for calculating the impedance profile is provided in [9]. Once the impedance profile is calculated, it is easy to sample it at any desired rate, and to solve the following nonlinear equations simultaneously to determine the patch width and height at any point along the length of the patch:

$$60\log\left[\frac{h}{w}\left\{6+0.2832\exp\left[-\left(30.666\frac{h}{w}\right)^{.7528}\right]\right\}+\sqrt{1+\left(2\frac{h}{w}\right)^2}\right]=Z_s,$$

where Z_s is the sampled impedance of the Klopfenstein profile, and

$$\frac{150}{f_l}=\frac{2}{\log\left[\frac{h}{w}\left\{6+0.2832\exp\left[-\left(30.666\frac{h}{w}\right)^{.7528}\right]\right\}+\sqrt{1+\left(2\frac{h}{w}\right)^2}\right]}.$$

5. Results of the Klopfenstein-Based MAMA

The simulated Klopfenstein design was operated at a starting frequency of 10 GHz. The profile was sampled at 10 points, and the maximum reflection coefficient in the pass band was specified to be 0.2. The ten points yielded the following patch profile:

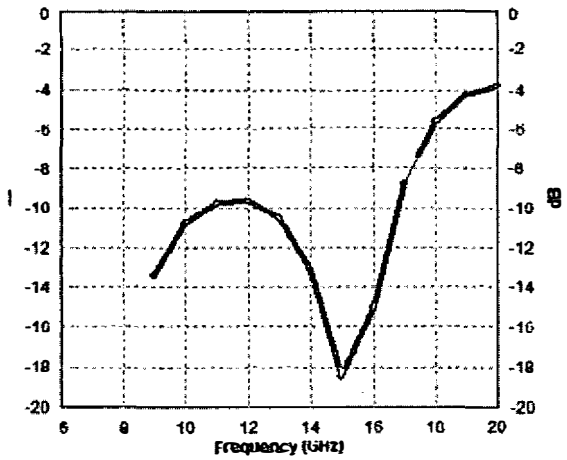

Figure 9a. The Klopfenstein MAMA $|S_{11}|$ parameters. The simulation results of the Klopfenstein MAMA showed its ability to comply with the designer's specifications, compared to the Chebyshev MAMA (i.e., comparing Figures 2-4 with Figure 9 showed similar results in terms of impedance bandwidth, total field gain, and antenna efficiency, despite the fact that the maximum reflection coefficient in the pass band was specified to be 0.2 for the Klopfenstein design, while for the Chebyshev MAMA an over-design had to be used to obtain the desired characteristics). The apparent reason for this is the smoothness of the Klopfenstein taper, compared to the sharp changes in the Chebyshev MAMA profile.

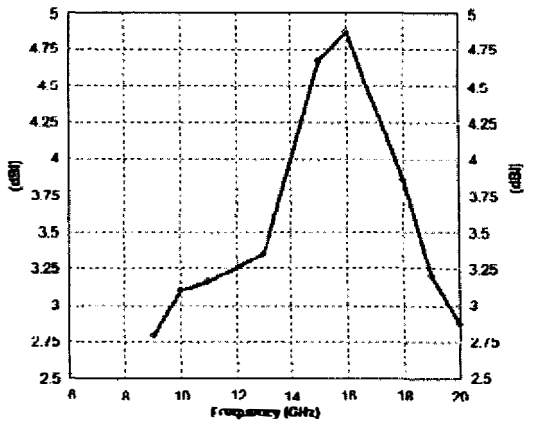

Figure 9b. The total Klopfenstein MAMA field gain. The other comments of Figure 9a apply.

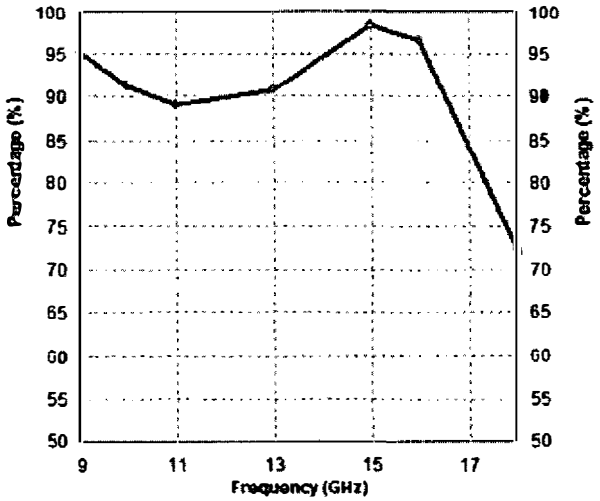

Figure 9c. The Klopfenstein MAMA efficiency. The other comments of Figure 9a apply.

$l = 0$ mm, $w = 9$ mm, $h = 2.4$ mm
$l = 1.0994513$ mm, $w = 68.849385$ mm, $w = 8.4$ mm, $h = 2.7$ mm
$l = 2.1989026$ mm, $w = 7.7$ mm, $h = 3.2$ mm
$l = 3.2983539$ mm, $w = 6.8$ mm, $h = 3.7$ mm
$l = 4.3978052$ mm, $w = 5.7$ mm, $h = 4.5$ mm
$l = 5.4972565$ mm, $w = 4.5$ mm, $h = 5.5$ mm
$l = 6.5967078$ mm, $w = 3.3$ mm, $h = 6.6$ mm
$l = 7.696159$ mm, $w = 2.3$ mm, $h = 8$ mm
$l = 8.7956103$ mm, $w = 1.5$ mm, $h = 9.4$ mm
$l = 9.8950616$ mm, $w = 0.9$ mm, $h = 10.9$ mm
$l = 10.994513$ mm, $w = 0.6$ mm, $h = 12.3$ mm

The $|S_{11}|$ parameters are shown in Figure 9.

The theoretical prototype for the Klopfenstein-based MAMA is given by

$$|S_{11}| = 20\log\left\{0.5\left(\ln\frac{Z_L}{Z_0}\right)\cos\frac{\left[\left(2\pi f\frac{L}{c}\right)^2-A^2\right]^{0.5}}{\cosh A}\right\}.$$

The dimensions of the ground plane were optimized to give the best possible bandwidth. The ground plane finally used had dimensions of 12.7 mm × 8.2 mm with the feed line at an offset of 1.35 mm to the right of the ground plane's midpoint on the x axis. From Figure 9, it was clear that although the specified maximum reflection for the Klopfenstein taper was higher than that for the Chebyshev taper, similar results were obtained. This showed that the Klopfenstein taper had a greater ability to conform to design specifications, which could be expected as a result of its smooth profile. However, this comes at the expense of ease of fabrication and an increase in antenna volume.

In an attempt to make the fabrication process easier, the authors proposed and implemented an alternative Klopfenstein-based scheme. To make the fabrication process easier, the values of w and h that satisfy the efficient radiation constraint and comply with the Klopfenstein taper were obtained through solving the following two equations, but only at the first and last point of the taper:

$$\frac{150}{f_0} = \frac{2}{\log\left[\frac{h}{w}\left\{6+0.2832\exp\left[-\left(30.666\frac{h}{w}\right)^{.7528}\right]\right\}+\sqrt{1+\left(2\frac{h}{w}\right)^2}\right]}$$

$$60\log\left[\frac{h}{w}\left\{6+0.2832\exp\left[-\left(30.666\frac{h}{w}\right)^{.7528}\right]\right\}+\sqrt{1+\left(2\frac{h}{w}\right)^2}\right] = Zklop_i$$

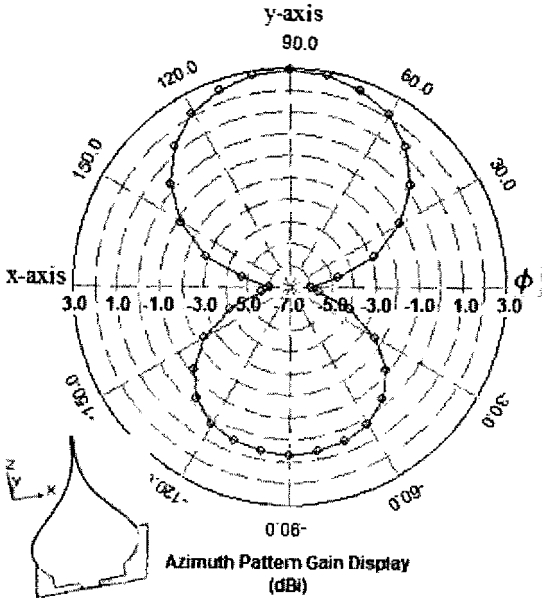

Figure 11a. The radiation pattern of the Klopfenstein MAMA in the xy plane. The pattern is shown at a frequency of 0.9 GHz. However, investigations of the patterns at other frequencies showed that the shape of the patterns did not change significantly with changes in frequency. However, there was a noticeable change in terms of gain level from the lower frequencies (from 1.0 to 1.5 GHz) to the higher frequencies (at 2 to 3 GHz).

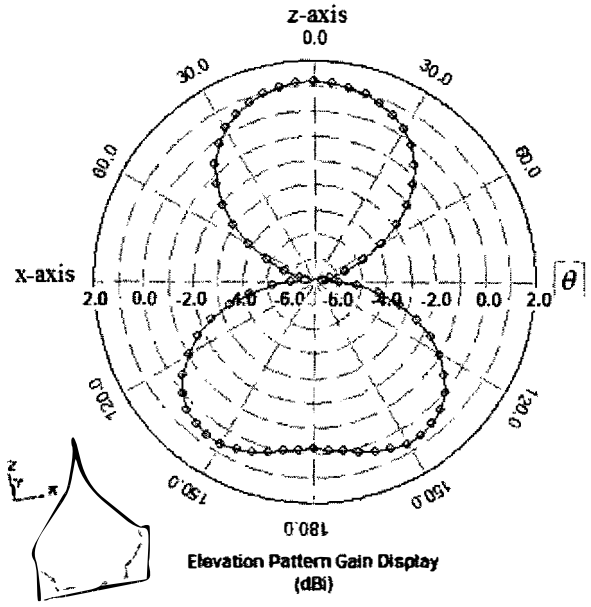

Figure 11b. The radiation pattern of the Klopfenstein MAMA in the xz plane. The other comments of Figure 9a apply.

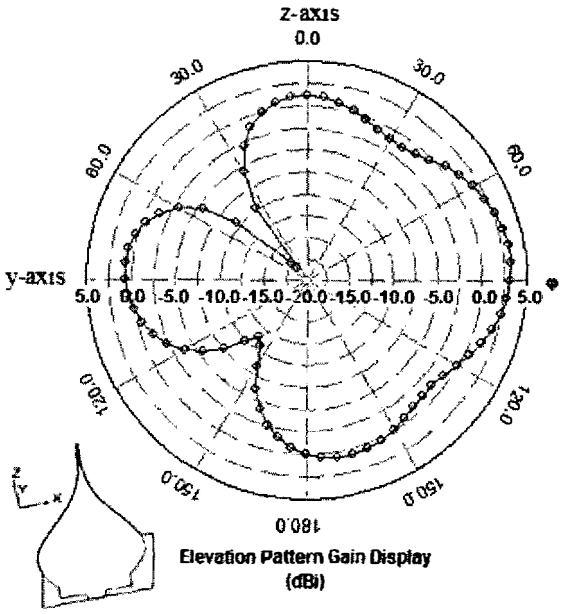

Figure 11c. The radiation pattern of the Klopfenstein MAMA in the yz plane. The other comments of Figure 9a apply.

where $Zklop_i$ is the Klopfenstein-taper impedance at sample point i. The two points obtained were then considered to be the trace of a plane parallel to the x axis. The whole Klopfenstein patch was then forced to lie within this plane (which inclined at angle θ, where $\tan\theta = \frac{\Delta z}{\Delta y}$). This was done by considering the height at each point known through the inclination angle of the plane through the simple relation

$$z = z_{initial} + \Delta y \tan\theta,$$

where $z_{initial}$ is the height at the initial sampling point of the Klopfenstein taper. Thus, only the width of the patch is left to determine, through

$$60\log\left[\frac{h}{w}\left\{6+0.2832\exp\left[-\left(30.666\frac{h}{w}\right)^{.7528}\right]\right\}+\sqrt{1+\left(2\frac{h}{w}\right)^2}\right] = Zklop_i$$

In the fabrication process, the antenna is first fabricated in the horizontal *xy* plane. Thus, the calculated parameters should be put into the format (w, $\frac{y}{\cos\theta}$). A suitable CAD program is then used to draw the 1-1 pattern of the Klopfenstein patch. After printing, this pattern is simply fixed by tape to a copper sheet and, using suitable scissors, an exact copy of the pattern in copper is fabricated. To adjust the inclination angle, the patch is supported at the beginning and middle using suitable dielectric rods, having heights equal to those calculated according to the inclination angle.

The authors used both *IE3D* and 602-suite programs to generate and print the 1-1 pattern. Figure 10 compares the simulation and practical results with the Klopfenstein MAMA prototype based on this approach. It was clear that in terms of bandwidth size, both the practical and simulation results were in perfect agreement. However, there were differences in the matching level between the simulation and practical results. The differences may have been due to several reasons. First, three small dielectric supports were used along the length of the Klopfenstein MAMA patch to keep it at the proper, calculated slope. Second, even with the dielectric support used, it was still quite difficult to maintain the feed height and patch inclination at the exact values deduced from the synthesis procedure. It is important to emphasize that these practical tolerances were left as they were intentionally to highlight the success of the Klopfenstein MAMA in achieving the prescribed broadband performance, even when constructed based on an inexpensive design procedure hampered with practical tolerances. The possibility of obtaining broadband performance using simple, inexpensive antennas was one of the main aims of the current thesis.

It is also clear from the figure that despite the smoothness of the Klopfenstein MAMA, the difference in the matching level between simulation and practical results and the synthesis prototype were still quite large. Possible causes for this were the following. First, the formula for the characteristic impedance used in the synthesis procedure was derived for the case of a rectangular patch, and this is not the case for a Klopfenstein MAMA. Moreover, since the Klopfenstein MAMA could be considered to be a series of patches, each having a length approaching zero, it was difficult to include the effective length in the same way as it was included for a rectangular patch. Third, as the height increased (the maximum height was at the tip of the patch), the possibility of the patch operating with higher-order modes increased, and consequently deviation from the TEM assumption on which the synthesis formulas were based occurred. However, from a practical point of view, all of these factors are not that important, as long as the antenna's performance (impedance bandwidth) was acceptable. Thus, adding complexity to the synthesis procedure to avoid these pitfalls is quite unjustified.

Figure 11 shows the radiation patterns of the Klopfenstein MAMA at 1 GHz. The patterns were considered to be omnidirectional and the effect of the finite ground plane was clear. The measured radiation patterns for both the Klopfenstein and Chebyshev MAMAs were done in an ordinary microwave lab (as opposed to an anechoic chamber), using the LabVolt antenna training kit. The measured patterns were in good agreement with the simulated results shown. The minor differences were easily

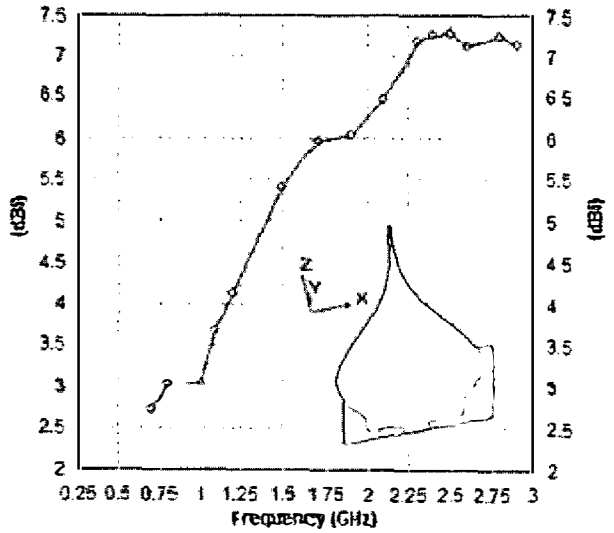

Figure 12a. The calculated total field gain of the fabricated Klopfenstein MAMA prototype. The gain ranged from 3 dBi to 7.25 dBi over the operating range.

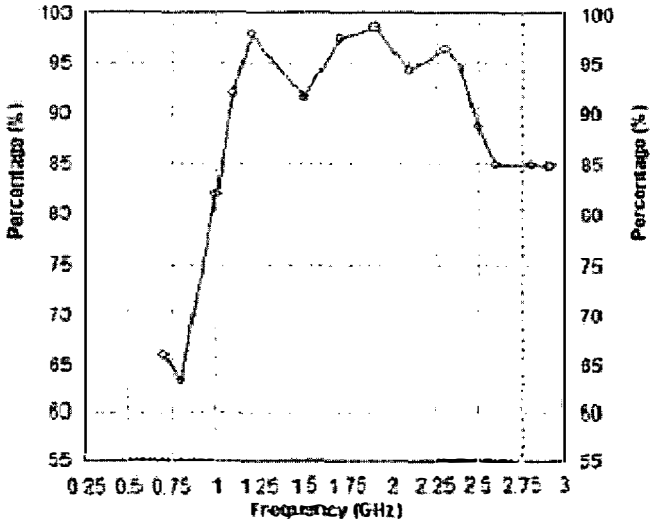

Figure 12b. The calculated efficiency of the fabricated Klopfenstein MAMA prototype. The efficiency ranged from 85% to 97% over the operating range.

accounted for, given the measurement setup, and understanding that the kit used was equipped with only a few support mechanisms that were not particularly ideal for maintaining the antennas in the correct position needed to get perfect agreement between experiment and simulation.

Figure 12 shows the total field gain and antenna efficiency (including the effect of the return loss, as well as losses due to surface waves) as a function of frequency. It was clear that the total field gain ranged from 3 dB to 7.25 dB, and that it increased with an increase in frequency. The antenna efficiency ranged from 85% to 97% over the operating bandwidth. This high efficiency was to be expected, due to the principle on which Klopfenstein MAMA was built, which ensured that the antenna was matched to both the feed line and to the air into which it radiated.

6. Conclusions

The present paper introduced a new class of broadband antennas, which combines the advantages of being simple to design and very easy and inexpensive to fabricate. The simplicity of the design procedure and of the resulting antenna structure are a result of the new formulation presented by the authors for the antenna design problem as an impedance-matching challenge. Thus, the authors hope that this paper encourages researchers to direct their attention to design procedures that have solid mathematical foundation, and that are liable to yield simple structures that can be easily fabricated from inexpensive components. As has been clearly demonstrated by this paper, these approaches are systematic, and can design simple, high-performance antennas, as opposed to the more complicated designs that are usually suggested by researchers at the present time, and which aim to achieve similar performance but at a much higher expense.

7. Acknowledgment

The authors would like to thank Zeland Support, especially Dr. Jian Zhang, for their support with the *IE3D* and *Fidelity* software.

8. References

1. K. Wong, *Compact and Broadband Microstrip Antennas*, New York, John Wiley and Sons, 2002.

2. G. Kumar and K. Ray, *Broadband Microstrip Antennas*, Norwood, MA, Artech House, 2003, pp. 383-384.

3. R. Garg, P. Bahartia, I. Bahl, and I. Ittipiboon, *Microstrip Antenna Design Handbook*, Norwood, MA, Artech House, 2001.

4. E. Hammerstad and O. Jensen, "Accurate Models for Microstrip Computer Aided Design," Symposium on Microwave Theory and Techniques, June 1980, pp. 407-409.

5. http://qucs.sourceforge.net/tech/node1.html

6. D. Pozar, *Microwave Engineering*, New York, John Wiley and Sons, 1998.

7. M. Kara, "Formulas for the Computation of the Physical Properties of Rectangular Microstrip Antenna Elements with Various Substrate Thicknesses," *Microwave and Optical Technology Letters*, **12**, 1996, pp. 234-239.

8. R. Klopfenstein, "A Transmission Line Taper of Improved Design," *Proceedings of the IRE*, **44**, January 1956, pp. 31-35.

9. M. Grossberg, "Extremely Rapid Computation of the Klopfenstein Taper," *Proceedings of the IEEE*, **56**, 9, September 1968, pp. 1629-1630.

Ideas for Antenna Designer's Notebook

Ideas are needed for future issues of the Antenna Designer's Notebook. Please send your suggestions to Tom Milligan and they will be considered for publication as quickly as possible. Topics can include antenna design tips, equations, nomographs, or shortcuts, as well as ideas to improve or facilitate measurements.